

The growing family of spatial solitons

G. I. STEGEMAN

Center for Research and Education in Optics and Lasers (CREOL) and Department of Physics,
University of Central Florida, 4000 Central Florida Blvd., Orlando, FL 32816-2700, USA.

The recent proliferation of spatial solitons which have been observed experimentally is discussed.

1. Introduction

The effects of material optical nonlinearities on the propagation of optical beams in nonlinear media have been investigated since the earliest days of nonlinear optics [1]. Self-focusing of laser beams, leading to beam filamentation and subsequently to material damage was frequently encountered. It was not until the 1970s that the connection was made between the one parameter family of solutions to the Nonlinear Schrödinger Equation (NLS), called solitons, and the observed beam filamentation and self-trapping [2]. These solutions are valid for 1D "pulses", *i.e.*, beams with a finite extent in one spatial or temporal dimension (time or space) travelling in a medium (Kerr) in which the self-induced index change Δn is strictly proportional to the local intensity I , *i.e.*, $\Delta n = n_2 I$. Solitons are robust, *i.e.*, not destroyed by small perturbations, and one parameter in the sense that choosing the peak power determines the pulse width, or vice-versa. In those early days, it was quickly realized that Kerr nonlinearities could only support stable spatial solitons with one transverse beam dimension, *i.e.*, in a slab waveguide. Later it was shown that an additional degree of freedom was required for the 2D case [1]. Stable self-trapped beams, but not solitons in the strictest mathematical sense, with two-dimensional (2D) cross-sections could also exist, but they required the presence of saturation in the index change with increasing intensity, or a higher order (*e.g.*, $\chi^{(5)}$) nonlinearity [1].

Although the initial interest in solitons was driven by the observed beam filamentation, it was temporal solitons that were first investigated experimentally in detail in glass fibres [3], [4]. Bright solitons were observed first [3]. They consist of an isolated bright temporal pulse which does not spread in time upon propagation. Later, dark solitons which correspond to a narrow intensity zero imbedded in a broad, background light field were observed [4]. This was followed by grey solitons for which the intensity goes to a minimum but not zero, the interactions between orthogonally polarized solitons, *etc.* [4], [5].

In this paper we will concentrate on spatial solitons and discuss the large variety of spatial solitons that have been observed experimentally to date, see Fig. 1. The

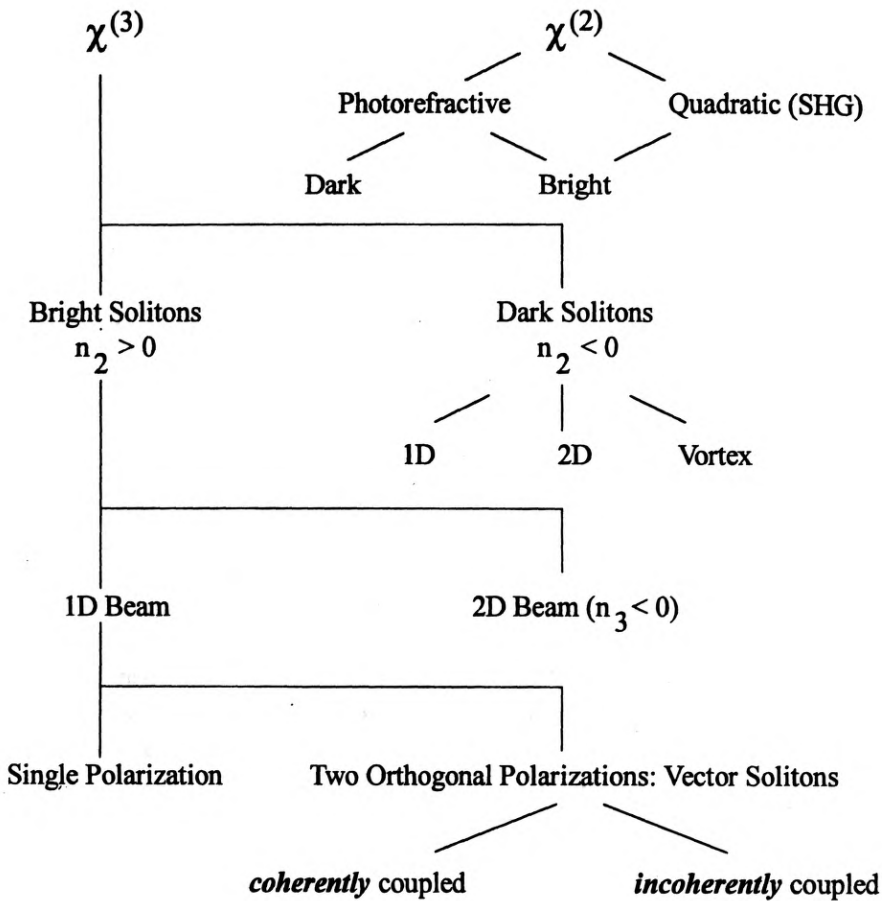


Fig. 1. Schematic of the spatial soliton family

first clean spatial solitons were observed in a waveguide made from CS_2 sandwiched by two glass plates in 1988 and this field has blossomed since then [6]. This paper is not meant to be a complete review. Instead the goal is to sketch the rich variety of spatial solitons that have been observed in the last few years.

2. Spatial solitons based on third order nonlinearities

Here there are three main categories of spatial solitons, bright, dark and vortex. Typical amplitude and phase distributions are shown in Fig. 2.

2.1. 1D bright spatial solitons

Bright spatial solitons were first identified in 1D CS_2 -filled slab waveguides. The nonlinearity was the classic intensity-induced molecular reorientation of optically anisotropic molecules. It resembles the Kerr case for small index changes [6]. These solitons are beams with a single polarization which propagate in a slab waveguide

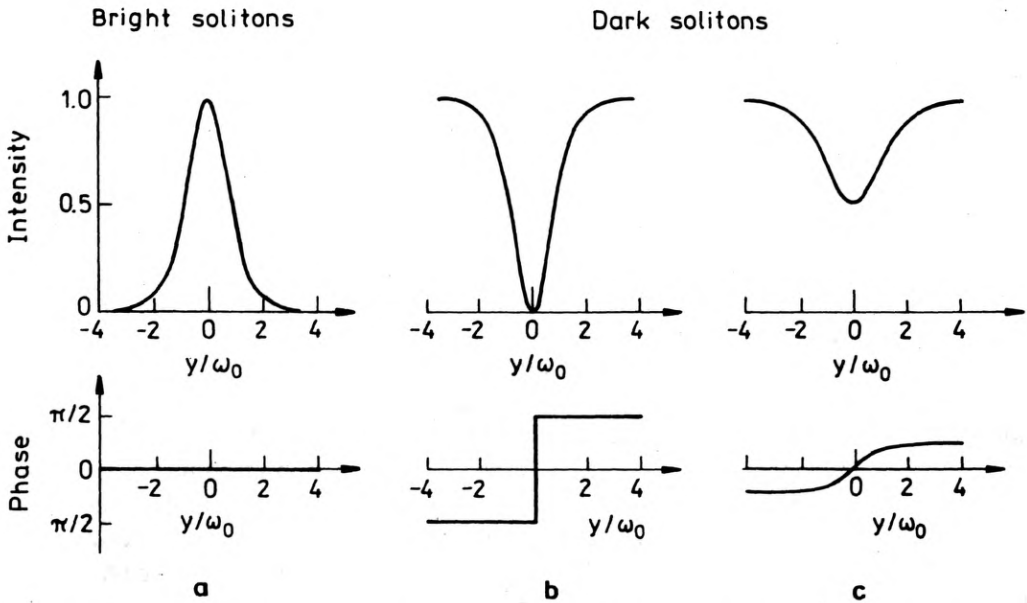


Fig. 2. Field amplitude and phase distributions associated with (a) a bright soliton, (b) a dark soliton and (c) a grey soliton

without spreading in the plane of the slab. For propagation along the z -axis and x normal to the slab surfaces, they satisfy the NLS equation

$$\frac{\partial E_e}{\partial z} = \frac{i}{2k} \frac{\partial^2 E_e}{\partial y^2} + ik_0 n_{2,E} |E_e|^2 E_e \tag{1}$$

where $n_2 > 0$ and we have assumed a TE guided mode (subscript e , a TM mode would be subscripted m). Note that the term $n_{2,E} |E_e|^2$ represents an intensity dependent refractive index change $\Delta n(I)$. This term is frequently called the self-phase modulation term. The solution, without the usual propagator term $\exp[i(\omega t - kz)]$, is of the form

$$E_e(\mathbf{r}) \propto \sqrt{\frac{n}{n_2 k \omega_0}} E_e(x) \operatorname{sech}\left(\frac{y}{\omega_0}\right) \exp\left[i \frac{z}{2k\omega_0^2}\right] \tag{2}$$

where ω_0 is approximately the $1/e$ beam halfwidth and $E_e(x)$ is the guided wave field distribution along x , the waveguide confinement axis. The corresponding field distribution is sketched in Fig. 2. For a pure n_2 nonlinearity, the solitons satisfy the NLS, and pass through each other on collision with no energy exchange. Ultrafast electronic Kerr nonlinearities were used first in glass and then later in AlGaAs waveguides to observe 1D spatial solitons [7], [8]. In all of these cases the soliton had a single polarization component.

Self-trapped beams, and even mathematical spatial solitons for a special case, can exist for dual polarization beams [9]–[11]. In 1996 dual polarization self-trapped

were observed for the first time [12], [13]. They satisfy the following equations for the two polarizations:

$$\frac{\partial E_e}{dz} = \frac{i}{2k} \frac{\partial^2 E_e}{\partial x^2} + ik_0 n_2 [|E_e|^2 E_e + A |E_m|^2 E_e + B E_m^2 E_e^* \exp(-2i\delta kz)], \quad (3)$$

$$\frac{\partial E_m}{dz} = \frac{i}{2k} \frac{\partial^2 E_m}{\partial x^2} + ik_0 n'_2 [|E_m|^2 E_m + A' |E_e|^2 E_m + B' E_e^2 E_m^* \exp(2i\delta kz)]. \quad (4)$$

Now in addition to the self-induced index change, there is also an index change induced by the orthogonally polarized component for each polarization. For example, for the TE polarization component, the TM induced index change is $n'_{2,E} |E_m|^2$, typically called cross-phase modulation. In the most general case, n_2 and $n'_{2,E}$, A and A' (ratio of cross-phase to self-phase modulation coefficients), and B and B' (coherent polarization coupling terms) are values appropriate to the TE and TM polarizations, respectively. The coupling terms lead directly to continuous, periodic with propagation distance, power exchange between the two polarizations. This results in "dynamic" spatial solitons since the beam widths of the two individual polarizations vary periodically with distance, but on the average the propagation is diffractionless. (There are also mixed polarization stationary solutions in which there is no power exchange, but these have not been found experimentally yet).

There is a special case called the Manakov soliton [9]. It is an integrable solution which requires very special material conditions, namely $n_2 = n'_{2,E}$, $A = A' = 1$ and $B = B' = 0$. In this case, the equations simplify to:

$$\frac{\partial E_e}{dz} = \frac{i}{2k} \frac{\partial^2 E_e}{\partial y^2} + ik_0 n_2 [|E_e|^2 + |E_m|^2] E_e, \quad (5)$$

$$\frac{\partial E_m}{dz} = \frac{i}{2k} \frac{\partial^2 E_m}{\partial y^2} + ik_0 n_2 [|E_m|^2 + |E_e|^2] E_m. \quad (6)$$

The unique nature of these Manakov solitons can now be seen from the term in the square brackets, the total induced index change which self-traps both polarizations equally. That is the soliton properties are independent of the fraction of power in each polarization.

The difficulty in generating Manakov solitons is due to a material with the right nonlinear properties. For example, an isotropic material cannot satisfy these conditions since $A = A' = 2/3$. Fortunately it was found that AlGaAs waveguides with the guiding material consisting of $\text{Al}_{0.18}\text{Ga}_{0.82}\text{As}$ for propagation along the [110] axis with the [001] axis normal to slab surfaces, satisfied $n_2 = n'_{2,E}$, $A = A' = 1$ to within the experimental uncertainty ($\pm 5\%$) [14]. Also, a trick was used to effectively make $B = B' = 0$. Namely, the TE and TM components were excited by two separate beams which had travelled through different optical elements and hence experienced different phase modulation, frequency chirping, etc. Therefore the two fields, each about 500 fsec long were no longer coherent with respect to each other, effectively eliminating the exchange coupling term. Experimentally it was found that

the soliton properties were independent of the fraction of power in the two polarizations, as long as the total power was a constant.

As shown in Figure 1, the bright, 1D, spatial solitons just discussed are just one branch of a large family of self-trapped beams. But, are these really all spatial solitons? In the strictest mathematical sense that a soliton is an integrable solution to the NLS equation, only the 1D single polarization and the incoherently coupled dual polarization beams are "solitons". In contrast, the coherently coupled dual polarization, 1D beam is a solitary wave, *i.e.*, a self-trapped beam. Nevertheless, it has now become common usage to call every self-trapped beam a soliton and we shall adopt this terminology here.

2.2. 2D bright spatial solitons

Beams with two transverse dimensions cannot form stable spatial solitons in pure Kerr law media. Another degree of freedom is needed. If the intensity-induced index change now takes on a more complicated (non-Kerr) form, namely $\Delta n = n_2 I + n_3 I^2$ with $n_2 > 0$ and $n_3 < 0$, then stable 2D solitons can exist. They are governed by

$$\frac{\partial E}{\partial z} = \frac{i}{2k} \frac{\partial^2 E}{\partial y^2} + \frac{i}{2k} \frac{\partial^2 E}{\partial x^2} + ik_0 \Delta n E. \quad (7)$$

No integrable solutions exist, but self-trapping does occur. A negative n_3 can occur physically from either a distortion in the potential well in which an electron sits, or via saturation in the population of an excited state generated by the incident light via absorption. Measurements of the nonlinear properties of the polydiacetylene bis-para-toluene sulfonate (PTS) at 1600 nm have shown exactly the right properties [15]. Because there was no measurable multiphoton absorption, it is unlikely that this nonlinearity is due to saturation. In fact, 2D spatial solitons have recently been observed in this material [16]. Another useful material system is a gas of atoms which can be approximated by two level systems for frequencies near an electronic transition [17].

2.3. Dark spatial solitons

As indicated previously in Figure 1, a negative Kerr nonlinearity ($n_2 < 0$) allows the excitation of dark spatial solitons. The appropriate 1D equation is Eq. (1). The stable solution for the defocusing case is

$$E_e(\mathbf{r}) \propto \sqrt{\frac{n_0}{|n_2|}} E_e(x) \tanh\left(\frac{y}{\omega_0}\right) \exp\left[i \frac{k_0 \Delta n}{n_0} z\right]. \quad (8)$$

Note that, as indicated in Figure 2, such a dark soliton requires a π phase shift at the zero in intensity. The dark soliton consists of an intensity zero which propagates without spreading, imbedded in a bright field of infinite extent. If in fact the launching conditions lead to a phase change of less than π , then the minimum does not reach zero and "grey" solitons are obtained.

True 1D dark spatial solitons have proven difficult to achieve experimentally.

Just as was the case for bright solitons, it is known that 2D dark solitons are unstable in bulk Kerr media, but are stable in saturable media [18]. Furthermore, if diffraction in one of the dimensions can be arrested, for example by diffraction from a periodic structure, the 2D case can be reduced to 1D [19]. The generating equations are essentially the same as those for 2D bright solitons, *i.e.*, Eq. (7) with $n_2 < 0$ and $n_3 > 0$. Such 2D dark spatial solitons have been generated in a number of different media, including liquids with thermal nonlinearities, semiconductors and gases (near a two level resonance) [19]–[21]. Although none of these cases really corresponded to local instantaneous nonlinearities, the observed beams were indistinguishable from dark and grey solitons. Note that it is not really feasible to produce an infinite background field into which the dark soliton is embedded because this requires infinite energy. Thus, in practice, the background field was of finite extent and in fact diffracted upon propagation, increasing with propagation distance the dark soliton width. This ultimately leads to the decay of a dark soliton into grey solitons.

A line array of dark spatial solitons has also been generated using a thermal nonlinearity [22]. Two weakly focused elliptical beams were intersected at a small angle to produce an interference pattern. This interference pattern evolved with distance into an array of regularly spaced dark solitons. The "gain" provided by the weak focusing was sufficient to prevent this 1D array of spatial solitons from reconstituting itself back into the interference pattern. The net result was a line of regularly spaced dark solitons.

4.4. Vortex solitons

One of the most interesting spatial soliton phenomena to be observed are vortex solitons [23]–[25]. A vortex in general is a singular point in space which has the property that integration of the phase of the electromagnetic field around this point yields a non-zero value, $\pm 2m\pi$, where m is an integer and the sign determines the sign of the "topological charge". What separates a vortex soliton from a linear vortex is its non-diffracting nature with propagation distance. The generating equation is again Eq. (7), but of course the boundary conditions at the input contain a screw discontinuity, *i.e.*, a vortex. Furthermore, another wave of either orthogonal polarization or at a different frequency can be guided in the vortex, *i.e.*, it acts like an optical fiber.

Dark vortex solitons have been generated directly with appropriate phase masks in both liquids (thermal nonlinearities), and in gases of two level atoms with an appropriate detuning from resonance to produce a defocusing nonlinearity [23], [24]. The field distribution is given approximately by [23]

$$E(\mathbf{r}, 0) \propto \sqrt{\frac{n_0}{|n_2|}} \tanh\left(\frac{R}{R_0}\right) \exp\left[i \frac{k_0 \Delta n}{n_0} z \pm i\Phi\right]. \quad (9)$$

Pairs of dark vortex solitons can also be generated by the modulational instability of a 1D dark stripe in an intense 2D background optical field of limited

extent [24]. This stripe first evolves into a "snake" instability. This, in turn, degenerates into pairs of dark vortex solitons which rotate around each other on further propagation. This beautiful demonstration is in excellent agreement with theory [24].

The generation of bright spatial solitary waves has also been observed by the break-up of an optical vortex in a saturable self-focusing medium [25]. A vortex imbedded in a strong bright field undergoes azimuthal symmetry breaking modulational instabilities. The resulting pairs of bright spatial solitons spiral around the center of the initial bright beam.

3. Solitons in quadratically nonlinear media

Spatial solitons have been observed which do not even require the traditional third order nonlinearities. For example, a variety of bright and dark spatial solitons have been reported in photorefractive media. And solitons even occur during second harmonic generation (SHG).

3.1. SHG solitons

These are a particular example of parametric solitons which can exist when fields at different frequencies are strongly coupled via a second order nonlinearity $\chi^{(2)}$ near phase-matching for that mixing interaction. The simplest case is for Type I SHG in which one fundamental beam produces one SHG beam. The usual coupled mode equations describe this process, namely:

$$\frac{d}{dz} E_1 = \frac{i}{2k_1} \frac{\partial^2 E_1}{\partial x^2} + \frac{i}{2k_1} \frac{\partial^2 E_1}{\partial y^2} - i\kappa(-\omega; 2\omega, -\omega) E_2 E_1^* \exp[i\Delta k z], \quad (10)$$

$$\frac{d}{dz} E_2 = \frac{i}{2k_2} \frac{\partial^2 E_2}{\partial x^2} + \frac{i}{2k_2} \frac{\partial^2 E_2}{\partial y^2} - i\kappa(-2\omega; \omega, \omega) E_1^2 \exp[-i\Delta k z], \quad (11)$$

where E_1 and E_2 are the complex field amplitudes for the fundamental and second harmonic, respectively, the wavevector mismatch is $\Delta k = 2k_1 - k_2 = 2k_{\text{vac}}(\omega)[n_1(\omega) - n_2(2\omega)]$ and κ is a coupling constant proportional to $d_{\text{eff}}^{(2)}$. The first two terms on the RHS are the usual diffraction terms and the third term describes the coupling which both regenerates the fundamental from the second harmonic (down-conversion in Eq. (10)) and generates the second harmonic (up-conversion) in Eq. (9).

Since there is no index change associated with this interaction, the origin of the beam narrowing effect is not immediately clear. Starting from the fundamental, the spatial width of the generated harmonic is spatially narrower than the fundamental because it is proportional to the fundamental spatial distribution squared. Similarly, the regenerated fundamental is narrower than the original fundamental for the same reason. The key condition for defeating diffraction is that the parametric gain length, defined by $|\kappa E_{1,2}|^{-1}$ is smaller than the diffraction length. This of course does not

guarantee a stable soliton solution. However, a stable soliton does evolve under those conditions.

Both 1D and 2D quadratic bright spatial solitons have been observed experimentally [26], [27]. Both are stable. For the 1D case investigated in LiNbO₃ slab waveguides, the SHG process was far from the phase-matching condition so that the second harmonic field was small [26]. The resulting spatial soliton closely resembled that of a Kerr 1D soliton.

The 2D spatial solitons during SHG have also been observed in bulk KTP which requires Type II phase-matching [27]. That is, two orthogonally polarized fundamental input beams are required. Above the threshold power, the three beams, two fundamental and one harmonic lock together in space and propagate together without diffraction. There are two additional features which make these spatial solitons especially useful. First, in situations with walk-off, *i.e.*, where the group velocities of at least one of the interacting beams is different from the other(s), all of the beams co-propagate above the soliton locking threshold, that is, no walk-off occurs. In addition, when the crystal alignment is not exactly at the phase-matching condition, the locking process "pulls" it onto phase-matching.

3.2. Photorefractive solitons

A variety of bright and dark spatial solitons can exist in photorefractive media. Absorption of light generates carriers whose motion, usually under the influence of an external field, leads to an internal electric field. The electro-optic effect then creates a refractive index change under the influence of the total local electric field. A "waveguide" is formed by the refractive index changes which then guide the beam itself, or other optical beams. The generic equation in 2D is

$$\frac{\partial E}{\partial z} = \frac{i}{2k} \frac{\partial^2 E}{\partial x^2} + \frac{i}{2k} \frac{\partial^2 E}{\partial y^2} + i \frac{k}{n} \Delta n(E) E \quad (12)$$

where the exact form of Δn determines the type of soliton obtained. Namely:

1. $\Delta n \propto r_{\text{eff}} [d^2 I / dy^2] / I$, where I is the optical intensity distribution gives a quasi-steady state photorefractive soliton [28]–[30]. Photocarriers are excited by optical absorption and carrier drift in the presence of an electric field establishes a screening field. During this process the ensuing gradients lead to a transient spatial soliton.

2. $\Delta n \propto r_{\text{eff}} I / [I + I_d]$, where I_d is the dark current leads to photovoltaic spatial solitons [31]. The index change required for these steady state solitons is generated by photovoltaic currents generated by the absorption of the light.

3. $\Delta n \propto r_{\text{eff}} / [I + I_d]$ leads to steady state screening solitons [32], [33]. In this case the photoexcited charge leaves the illuminated region under the influence of an external field, sets up its own internal field which at least partially compensates the external field in the illuminated region. Depending on the sign of the electric fields, electro-optic coefficients, and crystal orientation, the index change can lead to either dark or bright spatial solitons.

Which type of soliton can be excited depends on the details of the material properties (photovoltaic versus photoconductive, sign of electro-optic coefficients, etc.), and the conditions under which the external fields were applied. These solitons also have their stability criteria. For example, dark stripes on a 2D bright background have been shown to develop snake instabilities and to degenerate into pairs of optical vortices [34].

4. Summary

Eight years ago spatial solitons were reported for the first time in CS₂ slab waveguides. These were 1D bright solitons, based on a classical Kerr nonlinearity, stable solutions to the NLS equation. Since then the variety of spatial solitons has exploded. There are now solitons with more than one polarization in Kerr media, 2D spatial solitons based on saturable third order, or higher order nonlinearities, and single polarization, vortex and arrays of dark spatial solitons. A new branch has also been born, spatial solitons based on second order nonlinearities. These include different types of photorefractive spatial solitons, both bright and dark. And most remarkable are the quadratic spatial solitons which occur during parametric processes such as second harmonic generation. It has been truly an exciting time for spatial soliton physics.

Acknowledgements — This research was supported by the US National Science Foundation, Army Research Office and Air Force Office of Scientific Research.

References

- [1] For an early review see, AKHMANOV S. A., KHOKHLOV R. V., SUKHORUKOV A. P., Chapter in *Laser Handbook*, [Ed.] F. T. Arecchi and E. O. Schulz-DuBois, North-Holland, Amsterdam 1972, pp. 1151–1228.
- [2] ZAKHAROV V. E., SHABAT A. B., *Sov. Phys. JETP* **34** (1972), 62.
- [3] MOLLENAUER L. F., STOLEN R. H., GORDON J. P., *Phys. Rev. Lett.* **45** (1980), 1095.
- [4] WEINER A. M., HERITAGE J. P., HAWKINS R. J., Jr., THURSTON R. N., KIRSCHENER E. M., LEAIRD D. E., TOMLINSON W. J., *Phys. Rev. Lett.* **61** (1988), 2445.
- [5] Reviewed in: KIVSHAR Y. S., *IEEE J. Quantum Electron.* **29** (1993), 250.
- [6] MANEUF S., REYNAUD F., *Opt. Commun.* **66** (1988), 325.
- [7] AITCHISON J. S., WEINER A. M., SILBERBERG Y., OLIVER M. K., JACKEL J. L., LAIRD D. E., VOGEL E. M., SMITH P. W. E., *Opt. Lett.* **15** (1990), 491.
- [8] AITCHISON J. S., AL-HEMYARI K., IRONSIDE C. N., GRANT R. S., SIBBETT W., *Electron. Lett.* **28** (1992), 1879.
- [9] CHRISTODOULIDES D. N., JOSEPH R. L., *Opt. Lett.* **13** (1988), 53.
- [10] SNYDER A. W., HEWLETT S. J., MITCHELL D. J., *Phys. Rev. Lett.* **72** (1994), 1012.
- [11] AKHMEDIEV N. N., ELEONSKII V. M., KULAGIN N. E., SHILNIKOV L. P., *Sov. Tech. Phys.* **15** (1989), 587.
- [12] KANG J. U., STEGEMAN G. I., AITCHISON J. S., AKHMEDIEV N., *Phys. Rev. Lett.* **76** (1996), 3699.
- [13] AITCHISON J. S., KANG J. U., STEGEMAN G. I., *Power-dependent polarization dynamics of mixed-mode spatial solitary waves in AlGaAs waveguides*, to be published.
- [14] KANG J. U., STEGEMAN G. I., VILLENEUVE A., AITCHISON J. S., *AlGaAs below half bandgap: A laboratory for spatial soliton physics*, *J. European Opt. Soc., Part A*, in press.

- [15] LAWRENCE B., CHA M., KANG J. U., TORRUELLAS W., STEGEMAN G. I., BAKER G., METH J., ETEMAD S., *Electron. Lett.* **30** (1994), 447.
- [16] TORRUELLAS W., LAWRENCE B., STEGEMAN G. I., *Self-focusing and two-dimensional spatial solitons in PTS*, *Electron. Lett.*, submitted.
- [17] KONAR S., SENGUPTA A., *J. Opt. Soc. Am. B* **11** (1994), 1644, and references cited therein.
- [18] KROLIKOWSKI W., LUTHER-DAVIES B., *Opt. Lett.* **18** (1993), 188.
- [19] SWARTZLANDER G. A., Jr., ANDERSEN D. R., REGAN J. J., YIN H., KAPLAN A. E., *Phys. Rev. Lett.* **66** (1991), 1583.
- [20] LUTHER-DAVIES B., XIAOPING Y., *Opt. Lett.* **17** (1992), 496.
- [21] SKINNER S. R., ALLAN G. R., ANDERSEN D. R., SMIRL A. L., *IEEE J. Quantum Electron.* **27** (1991), 2211.
- [22] MAMYSHEV P. V., BOSSHARD C., STEGEMAN G. I., *J. Opt. Soc. Am. B* **11** (1994), 1254.
- [23] SWARTZLANDER G. A., Jr., LAW C. T., *Phys. Rev. Lett.* **69** (1992), 2503.
- [24] TIKHONENKO V., CHRISTOU J., LUTHER-DAVIES B., KIVSHAR Y. S., *Opt. Lett.* **21** (1996), 1129.
- [25] TIKHONENKO V., CHRISTOU J., LUTHER-DAVIES B., *J. Opt. Soc. Am.* **12** (1995), 2046.
- [26] SCHIEK R., BAEK Y., STEGEMAN G. I., *Phys. Rev. A* **53** (1996), 1138.
- [27] TORRUELLAS W. E., WANG Z., HAGAN D. J., VAN STRYLAND E. W., STEGEMAN G. I., TORNER L., MENYUK C. R., *Phys. Rev. Lett.* **74** (1995), 5036.
- [28] DUREE G., SCHULTZ J. L., SALAMO G., SEGEV M., YARIV A., CROSIGNANI B., DIPORTO P., SHARP E., NEURGAONKAR R., *Phys. Rev. Lett.* **71** (1993), 533.
- [29] DUREE G., SALAMO G. A., SEGEV M., YARIV A., CROSIGNANI B., DIPORTO P., SHARP E., *Opt. Lett.* **19** (1994), 1195.
- [30] DUREE G., MORIN M., SALAMO G., SEGEV M., CROSIGNANI B., DIPORTO P., SHARP E., YARIV A., *Phys. Rev. Lett.* **74** (1995), 1978.
- [31] TAYA M., BASHAW M., FEJER M. M., SEGEV M., VALLEY G. C., *Phys. Rev. A* **52** (1995), 3095.
- [32] ITURBE CASTILLO M. D., MARQUEZ AGUILAR P. A., SANCHEZ-MONDRAGON J. J., STEPANOV S., VYSLOUKH V., *Appl. Phys. Lett.* **64** (1994), 408.
- [33] SHIH M.-F., SEGEV M., VALLEY G. C., SALAMO G., CROSIGNANI B., DIPORTO P., *Electron. Lett.* **31** (1995), 826.
- [34] MAMAEV A. V., SAFFMAN M., ZOZULYA A. A., *Phys. Rev. Lett.* **76** (1996), 2262.

Received November 27, 1996